ELSEVIER

Polymer Vol. 37 No. 7, pp. 1273–1280, 1996

0032-3861/96/$15.00+0.00

Thermoreversible gelation of syndiotactic polystyrene in benzene

Ch. Daniel, M. D. Deluca* and J.-M. Guenet†
Laboratoire d'Ultrasons et de Dynamique des Fluides Complexes, Université Louis Pasteur–CNRS URA 851, 4 rue Blaise Pascal, F-67070 Strasbourg Cedex, France

and A. Brûlet and A. Menelle
Laboratoire Léon Brillouin, CNRS-CEA, CEN Saclay, F-91191 Gif-sur-Yvette Cedex, France
(Received 16 February 1995; revised 14 June 1995)

The temperature–concentration phase diagram of syndiotactic polystyrene (sPS)/benzene gels establishes the existence of two compounds, C_1 and C_2, the stoichiometries of which, expressed as benzene molecules/monomer, are 4/1 (C_1) and 1/1 (C_2). C_1 is an incongruently-melting compound as it transforms into C_2 at about the boiling point of benzene. In both compounds the chains take on a 2_1 helical form. Neutron diffraction investigations confirm the existence of these compounds but also disclose that compound C_1 possesses a novel crystalline form. Neutron scattering experiments reveal that sPS chains can be described by worm-like statistics in the molten state while still retaining a conformation close to the 2_1 helix. It is suggested that helix stabilization occurs by means of benzene molecules intercalated between the phenyl groups as previously proposed for isotactic polystyrene. A molecular model is put forward. The neutron scattering curves obtained in the gel state, although smeared by strong interchain scattering, are consistent with the absence of chain folding. The link between the fibrillar morphology of the gel and helix stabilization is discussed.

(Keywords: thermoreversible gels; syndiotactic polystyrene/benzene; chain conformation)

INTRODUCTION

Since the report by Keller and co-workers[1,2] of the appearance of an unusual chain conformation in thermoreversible gels from isotactic polystyrene (iPS), many investigations have been devoted to this polymer in an attempt to understand the underlying gelation mechanism. In particular, the reason why fibrillar gels were produced in the place of chain-folded crystals puzzled the scientific community.

Whereas Keller and co-workers[2] considered a non-solvated 12_1, helical form, Sundararajan *et al.* proposed a solvated 12_1 form[3]. Conversely, on the basis of neutron diffraction data, Guenet[4] proposed another model which, although still considering helix solvation, consisted of a near-3_1 helix, namely the well-known form of iPS. Guenet argued that this helix, through the position of the phenyl groups, creates cavities that can house solvent molecules. The advantage of this model is that it can account for why solvents possessing nearly identical interaction parameters produce gels with differing thermal properties[5]: the shape and size of the solvent are key parameters. Yet, as iPS gels are only poorly organized, no diffraction data are available to confirm or invalidate the above model which relies essentially on circumstantial evidence, although some investigations based on nuclear magnetic resonance spectroscopy (n.m.r.) support this view[6]. It is worth adding that the above model can also explain why chain rigidity is considerably enhanced in the solvent where gels are formed: solvent molecules act as helix stabilizer, and thus prevent the chain from folding. This led Klein *et al.*[7,8] to conclude that gelation, namely the making of swollen fibrillar systems, occurs because the chain is rigid and thus cannot fold.

The recent successes in synthesizing syndiotactic polystyrene (sPS)[9–11] have opened new possibilities for understanding the gelation phenomenon, and, correspondingly, for testing the cavity model. In fact, the stable helical structures are not the same as those with iPS, which should imply differing gelation behaviour. Gelation of sPS has been reported in many solvents[12,13] although, according to Daniel *et al.*[14], it is of absolute necessity to define clearly what is meant whenever the term gel is used. Guenet has given a definition[15] that relies mainly on the existence of a fibrillar network, the formation or fusion of which proceeds via a first-order transition. Recently, Daniel *et al.*[14] have shown that some simple mechanical testing allows one to recognize a gel. They particularly show that the test-tube method (or turning the tube upside down to show the absence of flow) is not reliable. As a result, systems that do not flow but consist of a packing of spherulites cannot be considered a gel. In other words, the question is: why are fibrils produced that lead to the formation of a gel?

In this paper on the gelation of sPS in benzene, we will

* Also affiliated with Sheffield Hallam University, Department of Applied Physics, Pond Street, Sheffield S1 1WB, UK
† To whom correspondence should be addressed

attempt to show that helix solvation is a very important factor.

EXPERIMENTAL

Materials

Syndiotactic polystyrene samples, hydrogenated (sPSH) and deuterated (sPSD), were synthesized following the method of Zambelli and co-workers[10]. Their contents of syndiotactic diads as measured by n.m.r. were found to be >99%. Characterization was achieved by gel permeation chromatography in dichlorobenzene at 140°C, yielding the following data: $M_w = 4.3 \times 10^4$ with $M_w/M_n \approx 3.6$ for sPSD; $M_w = 1.03 \times 10^5$ with $M_w/M_n \approx 4.4$ for sPSH.

Protonated benzene and deuterated benzene (>99% deuterated) were purchased from Aldrich and used without further purification.

Techniques and sample preparation

Differential scanning calorimetry (d.s.c.). The gel thermal behaviour and phase diagrams were established by means of a DSC 30 apparatus from Mettler. Pieces of gel prepared beforehand in test-tubes were introduced into stainless steel pans that were hermetically closed. The gels were melted again in the d.s.c. pan prior to any measurements.

Neutron diffraction. Neutron diffraction experiments were carried out on G-6-1 located at Orphée (Laboratoire Léon Brillouin, Saclay, France). G-6-1 is a two-axis spectrometer equipped with a banana-type counter containing 400 cells with an angular resolution of 0.2°. A wavelength of $\lambda = 0.474$ nm is obtained by diffraction under Bragg's condition onto a graphite monocrystal. By rotation of the counter the q-range $2\,\text{nm}^{-1} \leq q \leq 25\,\text{nm}^{-1}$ was accessible. Counter normalization was achieved with a vanadium sample.

The samples were prepared in cylindrical quartz cells of 4 mm inner diameter. The desired quantities of polymer and solvent were introduced together with a small metallic sphere. The cell was sealed hermetically from the atmosphere, and then heated at 140°C so as to obtain a homogeneous solution. The purpose of the metallic sphere was to facilitate solution preparation by moving it backwards and forwards by cell tilting. The different samples were then quenched to room temperature so as to form the gel.

Infra-red spectroscopy (i.r.). I.r. spectra were obtained using a Nicolet 60SX FT-IR spectrometer equipped with an MCT detector and possessing a resolution of $2\,\text{cm}^{-1}$. Thirty-two scans were performed per spectrum. The samples were first prepared in hermetically-sealed test-tubes. The samples were rapidly transferred onto the KBr plates, squeezed and scanned. The whole operation took less than about 3 min, ensuring minimum benzene evaporation.

Small-angle neutron scattering (SANS). SANS experiments were performed on PACE camera located at Orphée (Laboratoire Léon Brillouin). On this camera the scattered neutrons are collected on a detector made up of concentric, regularly spaced rings. To a ring of radius r corresponds a scattering vector $q = 4\pi/\lambda \sin\theta/2$, where $\theta = \arctan(r/D)$ with D the sample-to-detector distance. This detector can be moved to different distances from the sample. A mechanical selector provides neutrons with a wavelength distribution characterized by a relative width at half-height, $\Delta\lambda/\lambda_m$, of about 10%. By using different sample-to-detector distances and $\lambda_m = 0.6$ nm, the available q-range was $0.1 \leq q \leq 2.5\,\text{nm}^{-1}$.

Samples were prepared in hermetically-sealed quartz cells into which the desired quantity of each constituent was introduced beforehand. The mixture was heated at 140°C until a clear, homogeneous solution was obtained. The gels, obtained by a rapid quench to room temperature, consisted of some deuterated chains embedded in a matrix composed of protonated polymer together with a mixture of deuterated benzene and protonated benzene. This solvent mixture had a volume fraction composition of 5.9% deuterated benzene and 94.1% hydrogenous benzene, so as to match the coherent scattering amplitude of the protonated polymer. Under these conditions a blank sample free of deuterated chains showed a virtually flat scattering of an incoherent nature over the whole scattering range. This signal was subtracted after the usual corrections from the intensity scattered by the deuterium-labelled samples so as to extract the coherent intensity arising from the deuterated chains.

As usual, the position-sensitive counter was calibrated by using a solvent which exhibited purely incoherent scattering (in the present case, *cis*-decalin). Under these conditions the absolute intensity, $I_A(q)$, is written:

$$I_A(q) = \frac{I_N(q)}{K} \tag{1}$$

where $I_N(q)$ is the intensity obtained after background subtraction and transmission corrections, and counter normalization. K is a constant which includes the contrast factor and is written:

$$K = \frac{4\pi\delta N_A T_{dec}(a_H - a_D)^2}{g(\lambda)m_0^2(1 - T_{dec})} \tag{2}$$

where N_A is Avogadro's number; m_0 is the monomer molecular weight; T_{dec} and δ are the transmission and thickness, respectively, of the *cis*-decalin sample; a_H and a_D are the scattering amplitudes of the polymer species and of the protonated polymer, respectively. $g(\lambda)$ is a corrective term which depends upon the neutron wavelength, the wavelength distribution and the camera. This parameter was determined by means of a method devised by Cotton[16].

RESULTS AND DISCUSSION

Gel samples prepared from sPS in benzene are highly transparent. Investigation by electron microscopy of sPS/benzene aggregates shows the existence of fibres of average radius 20 nm (ref. 14). According to a definition recently discussed by Daniel *et al.*[14], sPS/benzene systems fall into the category of physical, thermoreversible gels.

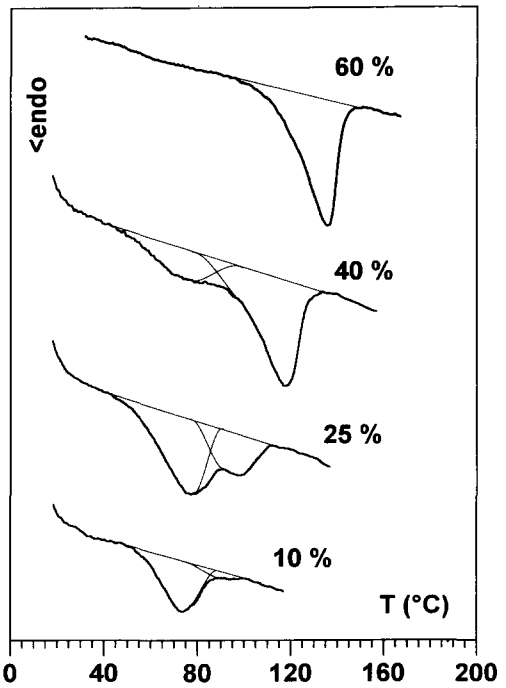

Figure 1 Typical d.s.c. traces obtained on heating sPS/benzene gels at $2°C\,min^{-1}$. Peak deconvolution is shown. Concentrations in w/w as indicated

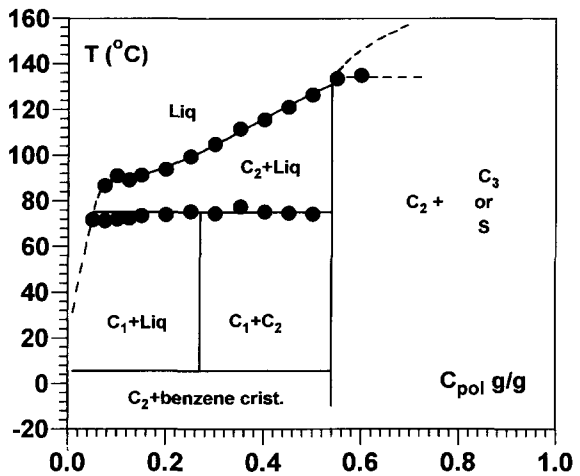

Figure 2 Temperature–concentration phase diagram for the system sPS/benzene. As is customary, full lines represent known transitions while dotted lines represent probable extensions

Thermal behaviour; temperature–concentration phase diagram

Because of limited sample availability, the d.s.c. investigation was carried out with the deuterated sPS sample. Typical d.s.c. traces are given in *Figure 1* for different polymer concentrations. As can be seen there are two endotherms, a low-melting endotherm and a high-melting endotherm. The temperature associated with the low-melting endotherm, T_{low}, is constant ($T_{low} = 75 \pm 3°C$), within experimental uncertainties, in the range of concentrations investigated. Conversely, the temperature associated with the high-melting endotherm, T_{high}, increases with increasing concentration. The phase diagram drawn in *Figure 2* highlights these different types of behaviour. Clearly, the

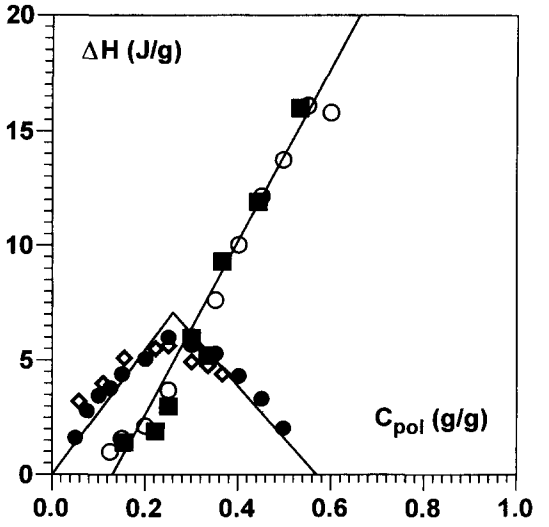

Figure 3 Enthalpies associated with various thermal events. On heating: ● = transformation $C_1 \Rightarrow C_2$ + liquid occurring at T_{low}; ○ = final melting endotherm. On cooling: ■ = first endotherm corresponding to the formation of C_2; ◇ = reaction C_2 + liquid $\Rightarrow C_1$

low-melting endotherm represents a temperature-invariant transition[17,18]. In *Figure 3* are represented the variation of the enthalpies associated with each endotherm as a function of polymer concentration. These enthalpies are obtained by performing a deconvolution of the endotherms as shown in *Figure 1*. This deconvolution is achieved by taking the onset of the second peak at the maximum of the first one.

The low-melting enthalpy first increases linearly up to a concentration $C_p = 0.26$, and then decreases linearly to become zero for $C_p = 0.57$. Conversely, the enthalpy of the high-melting endotherm increases continuously. The enthalpy variations together with the shape of the phase diagram are consistent with the existence of two compounds, C_1 and C_2, of different stoichiometries. C_1 is an incongruently-melting compound which transforms into C_2 at T_{low}. The reaction is written $C_1 \Rightarrow C_2$ + liquid at T_{low}. It is worth noticing that this transformation occurs very close to the boiling point of benzene (there is, however, no global solvent loss as the system is in a hermetically-sealed d.s.c. pan). The stoichiometry of compound C_1 is given by the maximum of the enthalpy associated with T_{low}, namely about 4 benzene molecules per monomeric unit. The stoichiometry of compound C_2 is obtained from the concentration at which the low-melting endotherm vanishes ($C_p = 0.57$), namely about 1 solvent molecule per monomeric unit. Due to the lack of data at higher concentrations it cannot be said whether C_2 is a congruently- or incongruently-melting compound.

The reverse transformation, namely liquid + $C_2 \Rightarrow C_1$, can be seen on cooling (see *Figure 4*). The first, high-temperature exotherm corresponds to the formation of compound C_2 while the second, low-temperature exotherm corresponds to the transformation of C_2 into C_1. The formation enthalpies corresponding to the high-temperature exotherm increase steadily with polymer concentration while those corresponding to the low-temperature exotherm go also through a maximum at about $C_p = 26\%$ (see *Figure 3*). Enthalpies determined on cooling and on heating are virtually identical as seen in *Figure 3*.

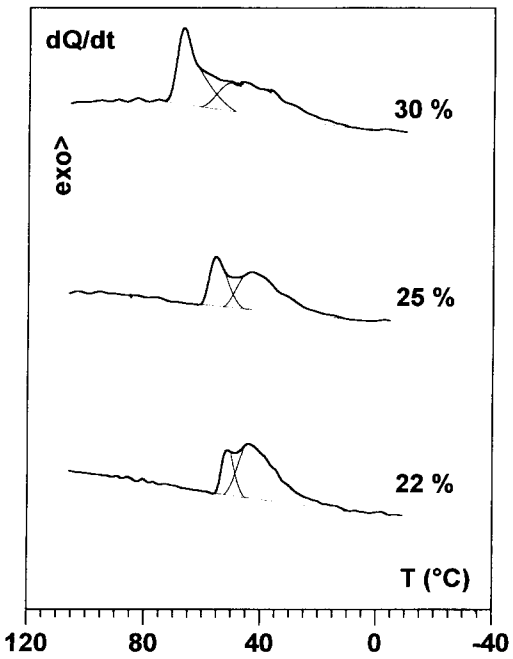

Figure 4 Formation exotherm obtained on cooling hot sPS/benzene solutions at 2°C min^{-1}. Peak deconvolution is shown. Concentrations as indicated

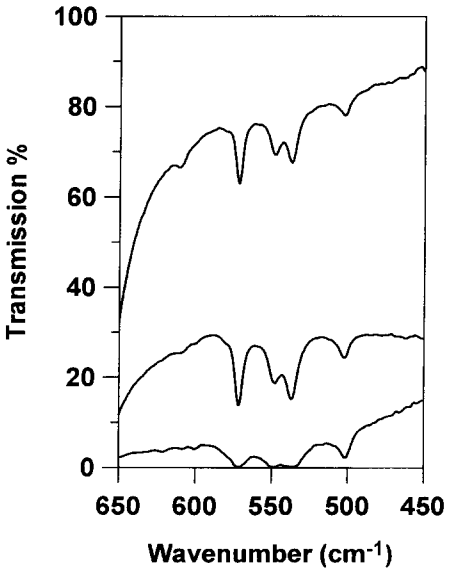

Figure 5 I.r. spectra of sPS/benzene gels: from top to bottom, $C_p = 2\%$, 26% and 40% (w/w)

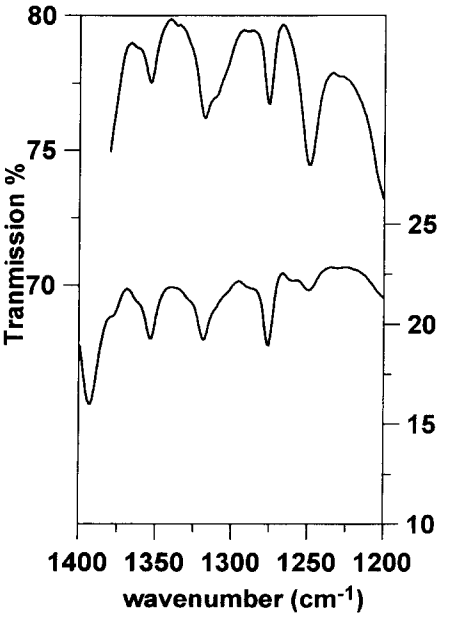

Figure 6 I.r. spectra of sPS/benzene gels: from top to bottom, $C_p = 2\%$ and 26% (w/w)

Studying the crystallization of benzene from the gel samples gives further information. The enthalpy associated with benzene melting decreases linearly with the gel polymer concentration (not shown here). It becomes zero for $C_p = 0.54$, a figure which turns out to be very close to that considered for the stoichiometry of compound C_2. In fact this is not mere coincidence: this type of study allows one to confirm the stoichiometry of compound C_2. Similarly, it shows that compound C_1 transforms into compound C_2 by crystallizing benzene. The fact that the transformation of compound C_1 into C_2 occurs either at a temperature close to boiling point of benzene or after benzene crystallization suggests two types of solvent molecules in compound C_1: those that are loosely bound and are therefore liable to be easily released (3 molecules/monomer) and those which are more tightly bound (1 molecule/monomer).

Beyond the concentration corresponding to the stoichiometry of compound C_2 no information is presently available, as it is quite difficult to prepare highly concentrated sPS/benzene solutions. We can only have a guess as to the phases involved. In the simplest situation, two cases are possible: either C_2 + solid (where the term 'solid' stands for a crystalline structure without solvent occluded) or $C_2 + C_3$.

The question as to whether the stoichiometry values derived from the phase diagram are relative or absolute deserves a short discussion. In other words, what is the effect of the amorphous content on the determination of these parameters? From the variation as a function of concentration of the enthalpy associated with the transformation occurring at T_{low}, the absolute stoichiometry is derived provided that the degree of crystallinity does not vary with polymer concentration. Under this assumption, the abscissae of both the maximum and the zero of the curve ΔH_T *versus* C_p are not dependent upon the degree of crystallinity. As a rule, the assumption of invariable crystallinity is valid within experimental uncertainties.

Molecular structure

The molecular structure consists of both the helical form taken on by the chains as well as the way they are packed. For sPS, a convenient way to find out what kind of helical structure is involved consists in performing an i.r. spectroscopy study since the two known helical forms[19–21], namely the zig-zag form and the 2_1 form, exhibit different spectra[12,22,23]. This method is better suited than any diffraction technique for which gel stretching would be necessary. As benzene is a very volatile solvent stretching could not be operated under proper conditions, and particularly not without altering the initial concentration.

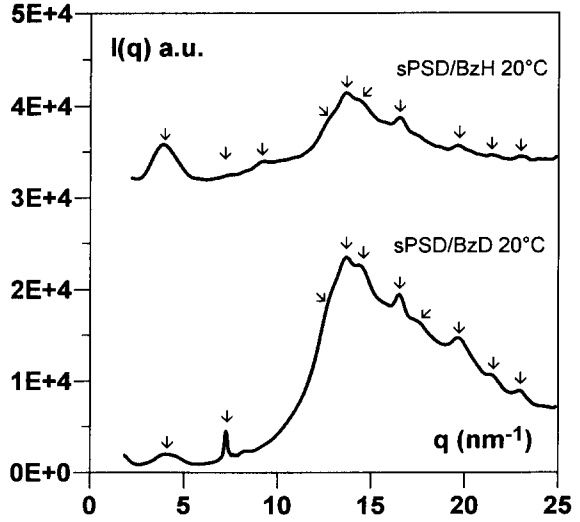

Figure 7 Neutron diffraction pattern for 26% gels (stoichiometry of compound C_1): top, deuterated polystyrene in hydrogenous benzene; bottom, deuterated polystyrene in deuterated benzene

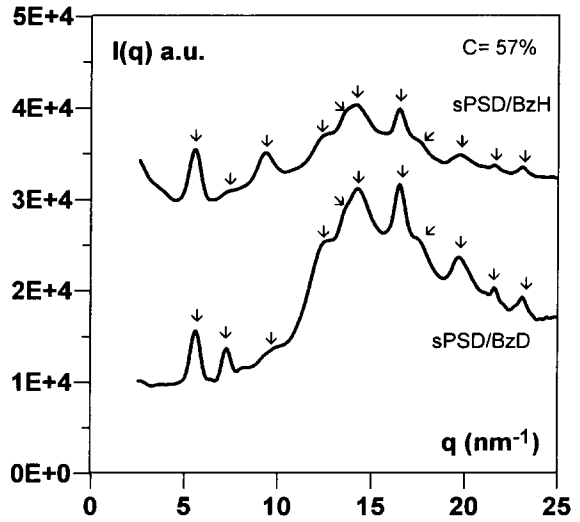

Figure 8 Neutron diffraction pattern for 57% gels (stoichiometry of compound C_2): top, deuterated polystyrene in hydrogenous benzene; bottom, deuterated polystyrene in deuterated benzene

The results are given in *Figures 5* and *6* for three different gel polymer concentrations: 2, 26 and 40%. As can be seen, in all three cases the i.r. spectra are consistent with the 2_1 form. This can be particularly seen in the range 500–600 cm^{-1} (*Figure 5*), where the three peaks characteristic of the 2_1 helix are seen, and also in the range 1250–1400 cm^{-1} (*Figure 6*), where the peaks at 1275, 1319 and 1353 cm^{-1} can be unambiguously attributed to this form. In no case do we observe any peak (537, 1224 and 1349 cm^{-1}) related to the planar zig-zag form. These results agree with previous findings by Kobayashi *et al.*[13]. We further show that C_1 and C_2 are characterized by the same helical form.

For gaining access to the way chains are packed, diffraction techniques are required. Neutron diffraction possesses many advantages when polymer–solvent compounds are dealt with[24]. This can be understood by considering the general expression for the intensity diffracted by a system containing two types of

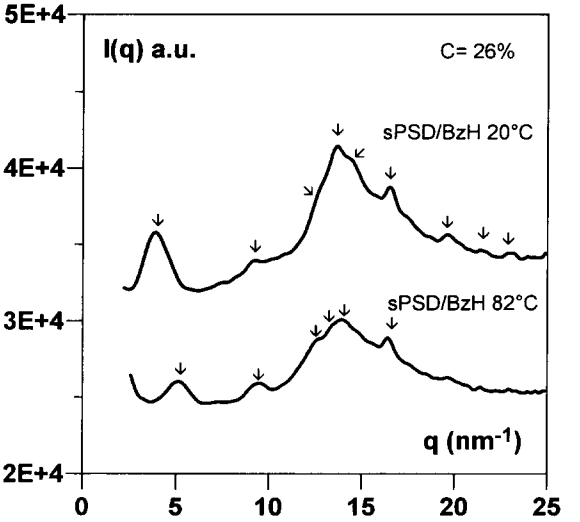

Figure 9 Neutron diffraction pattern for 26% gels (stoichiometry of compound C_1) composed of deuterated polystyrene and hydrogenous benzene: top, at 20°C; bottom, after heating to 82°C

molecule:

$$I(q) = K_p^2 S_p(q) + K_s^2 S_s(q) + 2K_p K_s S_{ps}(q) \qquad (3)$$

in which K and $S(q)$ are, with the appropriate subscripts, the contrast factor and the structure factor of the polymer and the solvent.

If the polymer crystallizes without solvent intercalation, then the cross-term can be neglected provided the crystal sizes are large enough. Changing the value of the contrast factor K_p of the polymer will affect the diffracted intensity, but by the same amount for all the diffraction peaks. Conversely, for polymer–solvent compounds, the cross-term must be taken into account. This entails that the diffracted intensities, and particularly the height of the diffraction peaks in relation to one another, will differ when using different labelling, i.e. modifying K_p and K_s. As a result, for neutron diffraction where both the solvent and the polymer can be either protonated or deuterated, four structure factors can be experimentally obtained.

Results presented in this paper will be interpreted in a qualitative way. A quantitative analysis for determining the crystalline lattice is in progress and will be reported in due course. Here, we discuss the results obtained at 20°C for gel polymer concentrations of 26 and 57% and at 82°C for gel polymer concentration of 26%.

As can be seen in *Figures 7* to *10*, the diffracted intensity differs with the differing labelling. For instance, all samples display a reflection at 7.2 nm^{-1} that is stronger for sPSD/benzeneD samples than for sPSD/benzeneH samples (*Figure 7*). This clearly indicates that benzene molecules are intercalated within the crystalline lattice. Moreover, these diffraction patterns also reveal that two compounds are dealt with, thus confirming the deductions drawn from the phase diagram. For sPSD/benzeneH systems one observes that the reflection at lowest q is significantly different. For the 26% sample the first reflection occurs at 3.9 nm^{-1} (*Figure 7*) as opposed to 5.1 nm^{-1} for the 57% sample (*Figure 8*). Otherwise, the other reflections are nearly the same. This result may suggest that one crystalline parameter of the crystalline lattice of compound C_1 is 'swollen' with respect to that of

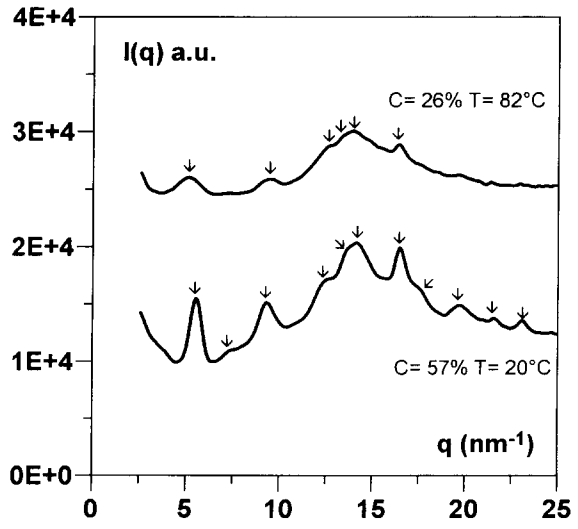

Figure 10 Neutron diffraction pattern for 26% gels (stoichiometry of compound C_1) after transformation at 82°C and 57% gels (stoichiometry of compound C_2) at 20°C. Both systems are deuterated polystyrene in hydrogenous benzene

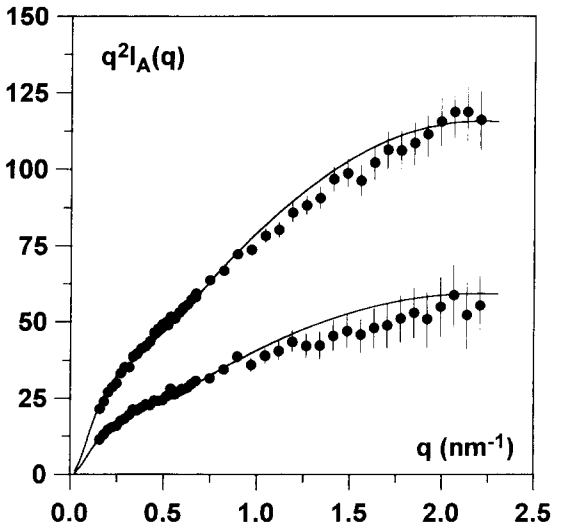

Figure 11 Neutron scattering curves represented by means of a Kratky plot [$q^2I(q)$ *versus* q]. Data obtained at two sample-to-detector distances. Top, $C_D = 6\%$; bottom, $C_D = 3\%$. The full lines represent the best fit obtained through the use of Yoshisaki and Yamakawa's relation[29]

compound C_2. Again, the outcome of this analysis is in agreement with the conclusions drawn from the temperature–concentration phase diagram: compound C_1 is more solvated than compound C_2. Another prediction from the phase diagram concerns the transformation occurring at 75°C. The diffraction patterns of a 26% sample at 20°C and 82°C reveal that a transformation has taken place (*Figure 9*): the reflection at 3.9 nm^{-1} has vanished whereas another one has appeared at 5.1 nm^{-1}. Evidently, the pattern at 82°C is quite similar to that obtained for a 57% sample which does confirm the reaction $C_1 \Rightarrow C_2 +$ liquid (*Figure 10*). It is worth emphasizing that the diffraction pattern observed here for C_1 has not been reported previously to our knowledge. A new crystalline form is therefore obtained under these conditions.

Of further note is the fact that the reflections are broad, which suggests either a rapid decorrelation between the lattice or small crystals. Both effects may come into play. The broadness of the reflections is possibly partially responsible for the apparent halo centred around $q = 14\,nm^{-1}$. Another origin for this halo together with reflection broadness may be due to decorrelation of the solvent molecules in the crystalline lattice which can then give rise to a liquid-type diffraction. The phase behaviour deduced from the phase diagram indicates that, at these concentrations, in no case can this halo arise from free solvent molecules such as would be found in isolated pockets of solvents.

Qualitatively, the results for C_2 are consistent with a lattice proposed by Chatani *et al.*[25] for the system sPS/toluene (monoclinic with $a = 1.758\,nm$, $b = 1.326\,nm$, $c = 0.771\,nm$, $\gamma = 121.2°$, space group $P2_1/a$). Yet, for the latter case, these authors suggest a stoichiometry of 1 toluene/4 monomer units, whereas the phase diagram here yields 1/1. As has been discussed in the previous section, the value of this stoichiometry is not overestimated. Provided that some adjustments are made to take this new stoichiometry into account, Chatani *et al.*'s lattice stands most probably as a good candidate. As will be discussed in the next section, there is still enough room to house additional solvent molecules. As for compound C_1, one probably has to contemplate a 'swollen' Chatani's lattice. The most ticklish issue remains the placement of the solvent molecules.

Chain conformation

The chain conformation was investigated in the gel state and in the molten state ($T = 121°C$) for an overall polymer concentration of 12%, corresponding to the system being under the C_1 compound structure. The overall concentrations of deuterium-labelled sPS were 6 and 3%. We first discuss the results obtained in the molten state that are drawn in *Figure 11* by means of a Kratky representation [$q^2I(q)$ *versus* q]. The scattering patterns can be easily fitted by using a worm-like chain model. According to Heine *et al.*[26] and Des Cloizeaux[27], for an infinitely long and infinitely thin Brownian chain characterized by a persistence length l_p, there exist two asymptotic regimes on either sides of a transfer momentum q^*:

$$\text{first asymptote} \qquad q^2 I_A(q) = \frac{6\mu_L}{l_p} \tag{4}$$

$$\text{second asymptote} \qquad q^2 I_A(q) = \mu_L \left[\pi q + \frac{2}{3l_p}\right] \tag{5}$$

q^* is then written

$$q^* = 16/3\pi l_p \simeq 1.7 \times l_p^{-1} \tag{6}$$

If the chain possesses a non-negligible transverse cross-section that is still smaller than the persistence length, then the q^{-1} behaviour shown in relation (5) will be altered in the following way (neglecting the constant term):

$$q^2 I_A(q) \simeq \pi \mu_L q f(qr_H) \tag{7}$$

In the case of a helical form of radius r_H, $f(qr_H)$ is written

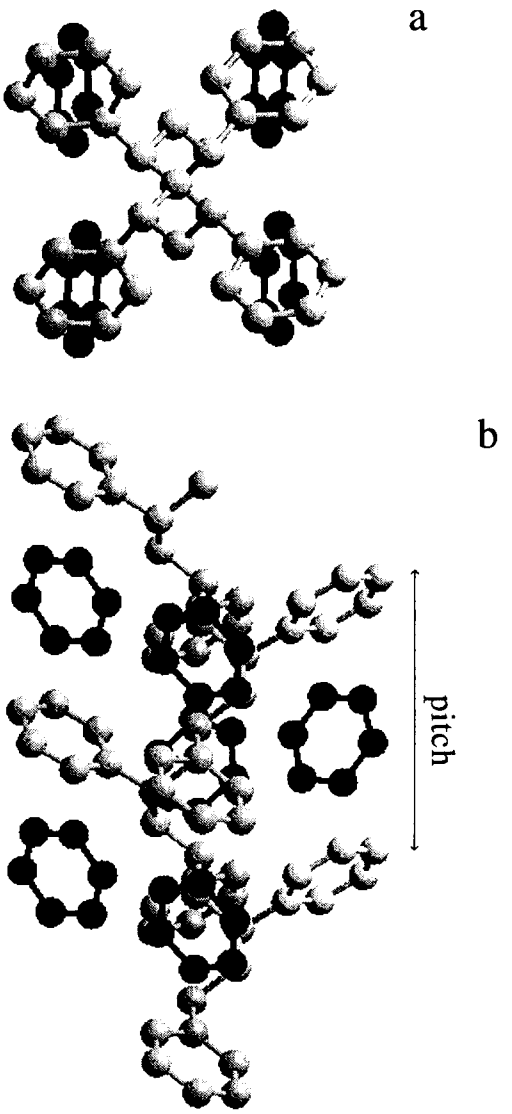

Figure 12 Possible location of a benzene molecules within the cavities created by phenyl rings when the chain takes on a 2_1 helical form: as seen (a) parallel to the *c*-axis, (b) perpendicular to the *c*-axis

at low resolution[28]:

$$f(qr_H) = \frac{4J_1^2(qr_H)}{q^2 r_H^2} \quad (8)$$

So far infinitely long chains have been considered. Yoshisaki and Yamakawa[29] have derived a semi-analytical expression for finite chains of contour length L for $ql_p < 5$. Their relations have been used here. To summarize, the fits given in *Figure 11* were performed with the following parameters: $L = 72\,\text{nm}$, $l_p = 4.8\,\text{nm}$, $r_H = 0.62 \pm 0.1\,\text{nm}$ and $\mu_L = 450\,\text{g nm}^{-1}\,\text{mol}^{-1}$.

The value of the persistence length indicates that sPS chains under these conditions are rather rigid, which is strongly reminiscent of what was observed for iPS in *cis*-decalin. The helix radius, $r_H = 0.62 \pm 0.1\,\text{nm}$, is consistent with a 2_1 helical form. This outcome together with the existence of local rigidity suggests therefore that the chains take on a near-2_1 form in the molten state of this system. As with iPS, the helical form is maintained well above the gel melting point. Again, this may indicate that solvent molecules stabilize the 2_1 helical form at this

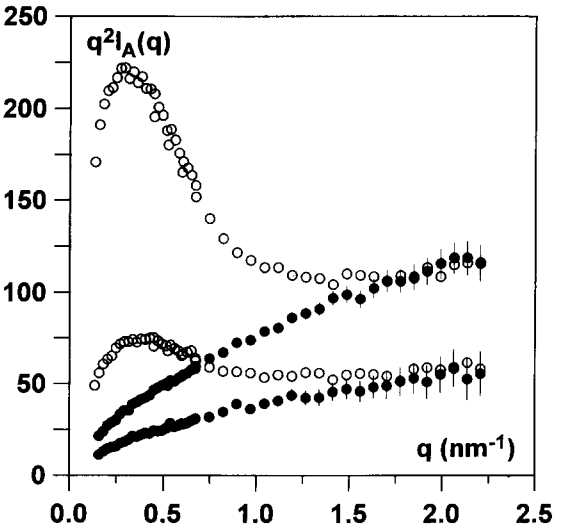

Figure 13 Neutron scattering curves represented by means of a Kratky plot [$q^2I(q)$ *versus* q]. Data obtained at two sample-to-detector distances. Top, $C_D = 6\%$; bottom, $C_D = 3\%$. Full circles represent the molten state and open circles represent the gel state

temperature. The model drawn in *Figure 12* seems to be worth considering. It turns out that the cavity created by sPS under the 2_1 form can house one benzene molecule under the orientation shown in *Figure 12*. This orientation is chosen by analogy with the arrangement of benzene molecules in their crystalline form[30,31]. In a benzene crystal one benzene molecule is intercalated between two other ones in the 101 plane so that molecules are perpendicular to one another (T-shape structure). The crystalline structure of benzene thus indicates that the type of interaction we are considering for benzene intercalated between the two phenyl groups is quite feasible. This model has two advantages: (1) it is certainly an efficient way to stabilize the 2_1 helical form; (2) if this solvation still exists in the gel (why should it not exist at lower temperature?), then this already provides a stoichiometry of 1 for compound C_2. This placement allows one to account for three very labile benzene molecules in compound C_1. Most probably, these three benzene molecules lie outside the helical form as there is no more room left. Their presence results in 'swelling' of the crystalline lattice. At the transformation temperature where $C_1 \Rightarrow C_2 + \text{liquid}$, these three molecules are expelled leaving only one benzene molecule. The model drawn in *Figure 12* is therefore consistent with the set of experimental results presented here.

It should be noted that, while the radius derived from the fit of the scattering curve does agree quite well with the theoretical radius of the 2_1 form, the value of μ_L is comparatively small since for deuterated chains one expects $\mu_L = 600\,\text{g nm}^{-1}\,\text{mol}^{-1}$. Experimental uncertainties only cannot account for this 30% discrepancy. The strong solvation of the chains of the type shown in *Figure 12* is a possible explanation for this effect. It is, however, difficult to quantify this effect as the use of a mixture of deuterated and hydrogenated benzene may complicate the question. Indeed, the composition of the mixture inside the helix is not necessarily the same as in the surrounding liquid. We shall leave this as an open question at the moment.

Investigation into the chain conformation in the gel

state does not provide one with clear-cut results; in fact, strong interchain interferences occur that smear the 'single' chain signal in the low q-range (see *Figure 13*). This interchain scattering is probably not due to isotopic segregation but arises from the fact that gelation takes place through a liquid–solid phase separation process. Under these conditions, there exist two well-defined phases: a polymer-poor phase and a polymer-rich phase. As most of the polymer is located in the polymer rich phase, the interchain pair radial distribution function is noticeably altered with regard to that of a homogeneous system (the liquid state for instance), particularly if the chains are highly parallel to one another, which results in the appearance of an additional signal. Only samples in which the deuterium-labelled chains were very diluted would be free of this phenomenon, but then the ratio signal/noise would be too small. This is not the case here as, for example, for a 6% deuterium-labelled sample one chain out of two is labelled in the organized domain. There is then no possibility to distinguish between a bunch of extended chains or folded chains. Clearly, future investigations have to be carried out at higher global polymer concentration using a lower amount of deuterated material.

In spite of these problems, some conclusions can be drawn from the present data. For both samples the intensity of the liquid state and the gel state are the same in the high q-range, which suggests identical structures at short distances. As it is known with certainty from the i.r. study that the chain takes on a 2_1 helix in the gel state, further support is given to the notion of conservation of the helical structure after gel melting. It cannot be said, however, whether the chain keeps its worm-like structure or tends to fold on itself in the gel state. The fact that in the liquid state, i.e. at high temperature where Brownian motion is important, the chain is worm-like would suggest that the same molecular morphology be at least preserved in the gel state. As stressed above, the fact that strong interchain scattering is observed may even suggest that chains are more rigid in the gel state. Indeed, only parallel rods are liable to produce high interscattering as is observed here[32].

If the analogy with iPS[7] is made, for which chain conformation is not altered after gel melting, then sPS chains must not fold in the gel state. Accordingly, sPS would give fibrillar gels because chain folding is impeded, and would therefore follow the empirical rule observed in many systems such as iPS[7] or agarose[33].

CONCLUDING REMARKS

Results presented in this paper establish clearly the formation of sPS/benzene compounds. Two compounds have been identified with differing stoichiometries: C_1 (4 benzene molecules/monomer), which is a newly observed crystalline form, and compound C_2 (1 benzene molecule/monomer). Compound C_1 contains 3 loosely-bound benzene molecules and 1 strongly-bound benzene molecule. Compound C_2 contains 1 strongly-bound benzene molecule. It is believed that this strongly-bound molecule is located within the cavity created by the phenyl rings when the chain is under a 2_1 helical form. This model can account for why the 2_1 helix is preserved in the molten state. As in many systems, sPS would then produce fibrillar physical gels owing to helix stabilization by the solvent which is liable to impede chain folding, and ultimately the formation of chain-folded crystals.

ACKNOWLEDGEMENTS

This work was supported by a grant from the EEC (Human Capital and Mobility Program) enabling the creation of a laboratories network entitled 'Polymer–solvent organization in relation to chain microstructure'.

The authors are indebted to Professor M. W. Hosseini for the use of molecular modelling programs, to Dr A. Thierry for the use of CERIUS programs and to Dr J. Druz for the use of the i.r. spectrometer.

REFERENCES

1 Girolamo, M., Keller, A., Miyasaka, K. and Overbergh, N. *J. Polym. Sci., Polym. Phys. Edn.* 1976, **14**, 39
2 Atkins, E. D. T., Isaac, D. H. and Keller, A. *J. Polym. Sci., Polym. Phys. Edn.* 1980, **18**, 71
3 Sundararajan, P. R., Tyrer, N. and Bluhm, T. L. *Macromolecules* 1982, **15**, 286
4 Guenet, J. M. *Macromolecules* 1986, **19**, 1960
5 Guenet, J. M. and McKenna, G. B. *Macromolecules* 1988, **21**, 1752
6 Nakaoki, T. and Kobayashi, M. *J. Mol. Struct.* 1991, **242**, 315
7 Klein, M., Brûlet, A. and Guenet, J. M. *Macromolecules* 1990, **23**, 540
8 Klein, M., Brûlet, A., Boué, F. and Guenet, J. M. *Polymer* 1991, **32**, 1943
9 Ishihara, N., Seimiya, Y., Kuramoto, M. and Uoi, M. *Macromolecules* 1986, **19**, 2464
10 Grassi, A., Pellechia, C., Longo, P. and Zambelli, A. *Gazz. Chim. Ital.* 1987, **19**, 2465
11 Pellechia, C., Longo, P., Grassi, A., Ammendola, P. and Zambelli, A. *Makromol. Chem. Rapid Commun.* 1987, **8**, 277
12 Prasad, A. and Mandelkern, L. *Macromolecules* 1990, **23**, 5041
13 Kobayashi, M., Nakaoki, T. and Ishihari, N. *Macromolecules* 1990, **23**, 78
14 Daniel, C., Dammer, C. and Guenet, J. M. *Polym. Commun.* 1994, **35**, 4243
15 Guenet, J. M. 'Thermoreversible Gelation of Polymers and Biopolymers', Academic Press, London, 1992
16 Cotton, J. P. in 'Neutron, X-ray and Light Scattering' (Eds P. Lindner and T. Zemb), Elsevier, 1991
17 Rosso, J. C., Guieu, R., Ponge, C. and Carbonnel, L. *Bull. Soc. Chim.* 1973, **9–10**, 2780
18 Koningsveld, R., Stockmayer, W. H. and Nies, E. *Makromol. Chem. Macromol. Symp.* 1990, **39**, 1
19 Immirzi A., De Candia, F., Ianelli, P., Zambelli, A. and Vittoria, V. *Makromol. Chem. Rapid Commun.* 1988, **9**, 761
20 Guerra, G., Vitagliano, V. M., De Rosa, C., Petraccone, V. and Corradini, P. *Macromolecules* 1990, **23**, 1539
21 Vittoria, V., Russo, R. and De Candia, F. *Polymer* 1991, **32**, 3371
22 Kobayashi, M., Ishihara, N. and Nakaoki, T. *Macromolecules* 1989, **22**, 4377
23 Vittoria, V. *Polym. Commun.* 1990, **31**, 263
24 Point, J. J., Damman, P. and Guenet, J. M. *Polym. Commun.* 1991, **32**, 477
25 Chatani, Y., Shimane, Y., Inagaki, T., Ijitsu, T., Yakinari, T. and Shikuma, H. *Polymer* 1993, **34**, 1620
26 Heine, S., Kratky, O., Porod, G. and Schmitz, J. P. *Makromol. Chem.* 1961, **44**, 682
27 Des Cloizeaux, J. *Macromolecules* 1973, **6**, 403
28 Pringle, O. A. and Schmidt, P. W. *J. Appl. Crystallogr.* 1971, **4**, 290
29 Yoshisaki, T. and Yamakawa, H. *Macromolecules* 1980, **13**, 1518
30 Cox, E. G. *Proc. R. Soc.* 1931, **A135**, 491
31 Bacon, G. E., Curry, N. A. and Wilson, S. A. *Proc. R. Soc.* 1964, **A279**, 98
32 Oster, G. and Riley, D. P. *Acta Crystallogr.* 1952, *5*, 272
33 Rochas, C., Brûlet, A. and Guenet, J. M. *Macromolecules* 1994, **27**, 3830